Inorg. Chem. **2007**, *46*, 9364–9371

Iron(III) Complexes with a Tripodal N_3O Ligand Containing an Internal Base as a Model for Catechol Intradiol-Cleaving Dioxygenases

Fei Li,[†] Mei Wang,*[,†] Ping Li,[†] Tingting Zhang,[†] and Licheng Sun*[,†,‡]

State Key Laboratory of Fine Chemicals, DUT-KTH Joint Education and Research Center on Molecular Devices, Dalian University of Technology (DUT), Dalian 116012, China, and Organic Chemistry, KTH Chemical Science and Engineering, Stockholm 10044, Sweden

Received April 6, 2007

A bis(μ-alkoxo)-bridged dinuclear iron(III) complex $[Fe(\mathbf{L})(NO_3)]_2(NO_3)_2$ [**1**; H**L** = *N*,*N*-bis(2-pyridylmethyl)-*N*-(2-hydroxyethyl)amine] of the tripodal N_3O ligand was prepared as a biomimetic model for the intradiol-cleaving dioxygenase enzymes. The reaction of **1** and catechol in the presence of excess triethylamine gave the catecholate (CAT) chelate bis(μ-alkoxo)-bridged dinuclear iron(III) complex $[Fe(\mathbf{L})(CAT)]_2$ (**2**). The molecular structures of complexes **1** and **2** were determined by X-ray crystallography. Diiron complexes **1** and **2** contain the same bis(μ-alkoxo)diiron diamond core. All heteroatoms (N_3O) of the ligand are coordinated to the iron center in complex **1** with two pyridine nitrogen atoms on the axial bonds, while one of the pyridyl arms of the ligand is left uncoordinated in complex **2**. The interaction of the diiron complex **1** and 3,5-di-*tert*-butylcatechol (H_2DBC) was investigated by electronic and mass spectroscopy. Complex **1** displays the intradiol-cleaving dioxygenase activity, and the coordinate ethoxyl arm of the ligand is capable of accepting the proton from catechol, which mimics the function of Tyr447 in the protocatechuate 3,4-dioxygenase as an internal base. The spectrophotometric titration experiment indicates the relatively low demand of the external base (0.8 equiv based on Fe^{3+}) for attaining the highest dioxygenase activity of complex **1**. The reaction rate of the reactive intermediate $[Fe(H\mathbf{L})(DBC)]^+$ with dioxygen is 0.38 M^{-1} s^{-1} determined by kinetic studies.

Introduction

In the past decades, mononuclear non-heme iron oxygenases have been intensively studied.[1−3] As one of the widely investigated non-heme iron enzymes, catechol dioxygenases are found in a diverse group of bacteria,[4−9] which can catalyze the oxidation of catechol to aliphatic acids using dioxygen as the oxidant with opening of the aromatic rings, either introdiol or extradiol cleavage.[10,11] The catechol intradiol-cleaving dioxygenases, such as catechol 1,2-dioxygenase and protocatechuate 3,4-dioxygenase (3,4-PCD), have attracted much attention. The X-ray crystal structure of as-isolated 3,4-PCD from *Pseudomonas putida* reveals a trigonal-bipyramidal iron(III) center coordinating with four endogenous protein ligands, namely, His460, His462, Tyr408, and Tyr447.[12−17] The fifth coordination position is occupied

* To whom correspondence should be addressed. E-mail: symbueno@dlut.edu.cn (M.W.), (L.S.).
[†] Dalian University of Technology.
[‡] KTH Chemical Science and Engineering.

(1) Que, L., Jr.; Ho, R. Y. N. *Chem. Rev.* **1996**, *96*, 2607.
(2) Costas, M.; Mehn, M. P.; Jenson, M. P.; Que, L., Jr. *Chem. Rev.* **2004**, *104*, 939.
(3) Kryatov, S. V.; Rybak-Akimova, E. V.; Schindler, S. *Chem. Rev.* **2005**, *105*, 2175.
(4) Gibson, D.T. *Microbial Degradation of Organic Molecules*; Marcel Dekker: New York, 1984.
(5) Que, L., Jr. In *Iron Carriers and Iron Proteins*; Loehr, T. M., Ed.; VCH: New York, 1989.
(6) Funabiki, T. *Oxygenase and Model System*; Kluwer: Dordrecht, The Netherlands, 1997.
(7) Bugg, T. D. H.; Winfield, C. J. *Nat. Prod. Rep.* **1998**, *15*, 513.
(8) Lange, S. J.; Que, L., Jr. *Curr. Opin. Chem. Biol.* **1998**, *2*, 159.
(9) Senda, T.; Sugiyama, K.; Narita, H.; Yamamoto, T.; Kimbara, K.; Fukuda, M.; Sato, M.; Yano, K.; Mitsui, Y. *J. Mol. Biol.* **1996**, *255*, 735.
(10) Solomon, E. I.; Brunold, T. C.; Davis, M. I.; Kemsley, J. N.; Lee, S.-K.; Lehenert, N.; Neese, F.; Skulan, A. J.; Yang, Y.-S.; Zhou, J. *Chem. Rev.* **2000**, *100*, 235.
(11) Feig, A. L.; Lippard, S. J. *Chem. Rev.* **1994**, *94*, 759.
(12) Que, L., Jr. In *Bioinorganic Catalysis*, 2nd ed.; Reedijk, J., Bouwman, E., Ed.; Marcel Dekker: New York, 1999.
(13) Ohlendorf, D. H.; Lipscomb, J. D.; Weber, P. C. *Nature* **1998**, *336*, 403.
(14) Ohlendorf, D. H.; Orville, A. M.; Lipscomb, J. D. *J. Mol. Biol.* **1994**, *244*, 586.
(15) Vetting, M. W.; Earhart, C. A.; Ohlendorf, D. H. *J. Mol. Biol.* **1994**, *236*, 372.
(16) Elgren, T. E.; Orville, A. M.; Kelly, K. A.; Lipscomb, J. D.; Ohlendorf, D. H.; Que, L., Jr. *Biochemistry* **1997**, *36*, 11504.

10.1021/ic700664u CCC: $37.00
Published on Web 10/05/2007

by a solvent-derived hydroxide ligand. On the basis of the crystallographic and spectroscopic studies, a substrate activation mechanism was proposed.[18,19] At the starting stage of the catalytic cycle, the hydroxide and the Tyr447 units act as Lewis bases to accept two protons of the catechol substrate and detach from the iron center to form an enzyme/substrate adduct.[20−23] Consequently, the coordinated substrate with semiquinonate radical character is attacked by dioxygen to form a peroxide intermediate. After a Criegee-type rearrangement of the peroxide intermediate, muconic anhydride is generated, which is further converted to ring-opened products.

Various non-heme iron complexes have been prepared as structural and functional models for catechol intradiol-cleaving dioxygenases to gain insight into mechanism of catechol oxidation and to explore their dioxygenase activity toward different catechol substrates.[2,24] A systematic research on iron(III) complexes with tris(2-pyridylmethyl)amine (TPA) tripodal tetradentate ligands has been done by Que et al.[19,25−27] The spectroscopic and kinetic studies on the catechol degradation promoted by the model complexes showed the relationship between the Lewis acidity of the iron center and its catechol dioxygenase activity. Among these model complexes, $[Fe(TPA)(DBC)]^+$ (H_2DBC = 3,5-di-*tert*-butylcatechol) was found so far to be the most active adduct in the intradiol-cleaving oxidation.[19] Krebs and coworkers reported model complexes with tetradentate ligands containing imidazole or benzoimidazole moieties and the dioxygenase activities of the model complexes toward H_2-DBC and other catechol substrates.[28−31] Although the catechol dioxygenase activities of iron complexes containing the phenolate units are normally lower than those with N_4 ligands,[24] they have received particular concern because a phenolate moiety can mimic the tyrosine residue around the iron center in 3,4-PCD. Many iron(III) complexes with mono- and bis(phenolate) tripodal ligands were reported.[25,26,32−38]

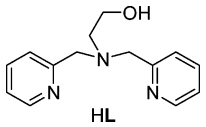

HL

Figure 1. Tripodal N_3O ligand H**L**.

By introduction of groups with different electronic or steric effects on the ligand, the Lewis acidities as well as dioxygenase activities of the complexes could be tuned.[33,34,36−38] In light of the bipyramidal configuration of 3,4-PCD, a five-coordinate complex $[Fe(Me_6\text{-Salen})(OH_2)](ClO_4)$ [Me_6-Salen = bis(3,5-dimesitylsalycilidene)-1,2-dimesitylethylenediamine] was prepared by Fujii and Funahashi.[39] Recently, an iron complex with the NMe_2 arm was also found to be in five-coordinate bipyrimidal coordination geometry.[37]

Krebs et al. found that the complex, generated in situ by $Fe(ClO_4)_3$ and the ligand (6-bromo-2-pyridylmethyl)bis(2-pyridylmethyl)amine (BrTPA), needed only 1.5 equiv of piperidine to attain the maximum reaction rate for the catechol oxidation, indicating that the bromopyridyl unit could act as an internal base analogous to Tyr447 in 3,4-PCD.[40] Yamahara et al. reported that the exogenous acetylacetonate (acac) ligand in iron(III) complexes served as 1 equiv of base upon catecholate coordination.[33] Inspired by theses results, we designed and studied functional models that can mimic the role of Tyr447 in the first step of catechol intradiol cleavage. Herein we report the preparation of a bis(μ-alkoxo)-bridged dinuclear iron(III) complex $[Fe(\mathbf{L})(NO_3)]_2(NO_3)_2$ [**1**; H**L** = *N*,*N*-bis(2-pyridylmethyl)-*N*-(2-hydroxyethyl)amine; Figure 1] with a tripodal tetradentate N_3O ligand. The ethoxyl moiety of ligand **L** is capable of mimicking the function of Try447 in 3,4-PCD for proton transfer from catechol to ligand. The species $[Fe(\mathbf{L})(OMe)]^+$, spontaneously derived from complex **1** in methanol, exhibits a moderate dioxygenase activity for catechol intradiol cleavage with a relatively low demand of an external base. The reaction of **1** and catechol in the presence of excess triethylamine gave a dinuclear iron(III) catecholate adduct $[Fe(L)(CAT)]_2$ (**2**; CAT = catecholate). The molecular structures of complexes **1** and **2** were characterized by X-ray analyses. The electronic property and reactivity of complex **1** in catechol degradation were investigated.

Experimental Section

Materials and Instruments. 3,5-Di-*tert*-butylcatechol (H_2DBC; 99%) was purchased from Acros. Other commercially available

(17) Vetting, M. W.; Ohlendorf, D. H. J. *Structure* **2000**, *8*, 429.
(18) Que, L., Jr.; Lipscomb, J. D.; Münck, E.; Wood, J. M. *Biochim. Biophys. Acta* **1977**, *485*, 60.
(19) Jang, H. G.; Cox, D. D.; Que, L., Jr. *J. Am. Chem. Soc.* **1991**, *113*, 9200.
(20) Vetting, M. W.; D'Argenio, D. A.; Ornston, L, N.; Ohlendorf, D. H. *Biochemistry* **2000**, *39*, 7943.
(21) Orville, A. M.; Elango, N.; Lipscomb, J. D.; Ohlendorf, D. H. *Biochemistry* **1997**, *36*, 10039.
(22) Orville, A. M.; Lipscomb, J. D.; Ohlendorf, D. H. *Biochemistry* **1997**, *36*, 10052.
(23) True, A. E.; Orville, A. M.; Pearce, L. L.; Lipscomb, J. D.; Que, L., Jr. *Biochemistry* **1990**, *29*, 10847.
(24) Yamahara, R.; Ogo, S.; Masuda, H.; Watanabe, Y. *J. Inorg. Biochem.* **2002**, *88*, 284.
(25) Que, L., Jr.; Kolanczyk, R. C.; White, L. S. *J. Am. Chem. Soc.* **1987**, *109*, 5373.
(26) Cox, D. D.; Benkovic, S. J.; Bloom, L. M.; Bradley, F. C.; Nelson, M. J.; Que, L., Jr.; Wallick, D. E. *J. Am. Chem. Soc.* **1988**, *110*, 2026.
(27) Cox, D. D.; Que, L., Jr. *J. Am. Chem. Soc.* **1988**, *110*, 8085.
(28) Duda, M.; Pascaly, M.; Krebs, B. *Chem. Commun.* **1997**, 835.
(29) Pascaly, M.; Duda, M.; Rompel, A.; Sift, B. H.; Meyer-Klaucke, W.; Krebs, B. *Inorg. Chim. Acta* **1999**, *291*, 289.
(30) Pascaly, M.; Nazikkol, Ç.; Schweppe, F.; Wiedemann, A.; Zuilinden, K.; Krebs, B. *Z. Anorg. Allg. Chem.* **2000**, *626*, 50.
(31) Pascaly, M.; Duda, M.; Schweppe, F.; Zurlinden, K.; Müller, F. K.; Krebs, B. *J. Chem. Soc., Dalton Trans.* **2001**, 828.
(32) Viswanathan, R.; Palaniandavar, M. *J. Chem. Soc., Dalton Trans.* **1995**, 1259.
(33) Yamahara, R.; Ogo, S.; Watanabe, Y.; Funabiki, T.; Jitsukawa, K.; Masuda, H.; Einaga, H. *Inorg. Chim. Acta* **2000**, *300−302*, 587.
(34) Merkel, M.; Müller, F. K.; Krebs, B. *Inorg. Chim. Acta* **2002**, *337*, 308.
(35) Nishida, Y.; Shimo, H.; Kida, S. *J. Chem. Soc., Chem. Commun.* **1994**, 1611.
(36) Viswanathan, R.; Palaniandavar, M.; Balasubramanian, T.; Muthiah, T. P. *Inorg. Chem.***1998**, *37*, 2943.
(37) Velusamy, M.; Palaniandavar, M.; Gopalan, R. S.; Kulkarni, G. U. *Inorg. Chem.* **2003**, *42*, 8283.
(38) Velusamy, M.; Malimurugan, R.; Palaniandavar, M. *Inorg. Chem.* **2004**, *43*, 6284.
(39) Fujii, H.; Funahashi, Y. *Angew. Chem., Int. Ed.* **2002**, *41*, 3638.
(40) Merkel, M.; Schnieders, D.; Baldeau, S. M.; Krebs, B. *Eur. J. Inorg. Chem.* **2004**, 783.

chemicals, ethanolamine, 2-picolyl chloride hydrochloride, and Fe(NO$_3$)$_3$·9H$_2$O were of reagent grade and were used as received.

The electronic absorption spectral measurements were made in methanol solutions of the complexes at ambient temperature (25 °C) with a HP (Hewlett-Packard) 8453 diode array UV−vis spectrophotometer. The ^{1}H NMR spectra were collected on a Varian INOVA 400-MHz apparatus with tetramethylsilane (TMS) as the internal standard. Mass spectrometry spectra were recorded either on an HP1100 LC/MSD instrument or on an HPLC-Q-TOF (Micromass, Wythenshawe, U.K.) mass instrument. Elemental analyses were performed on a Thermoquest-Flash EA 1112 elemental analyzer. Gas chromatography−mass spectrometry (GC−MS) analyses were carried out on an HP6890GC/5973MS apparatus equipped with a flame ionization detector (FID) and an HP-5 capillary column (30 m × 0.32 mm × 2.5 μm). The sample was run under the following conditions: initial temperature 100 °C; heating rate 10 °C min^{-1}; final temperature 220 °C; injection temperature 250 °C; FID temperature 250 °C.

Preparation of the Ligand. Ligand *N*,*N*-bis(2-pyridylmethyl)-*N*-(2-hydroxyethyl)amine (H**L**) was synthesized according to the literature procedure.[41]

Preparation of Iron Complexes. All reactions related to iron complexes were carried out under dry oxygen-free dinitrogen with standard Schlenk techniques. Solvents were dried and distilled prior to use according to the standard methods.

[Fe(L)(NO$_3$)]$_2$(NO$_3$)$_2$ (1). A methanol solution (5 mL) of Fe(NO$_3$)$_3$·9H$_2$O (0.30 g, 0.74 mmol) was added to a solution of H**L** (0.18 g, 0.74 mmol) in methanol (5 mL). The mixture was stirred for 1 h at room temperature. The solution was then concentrated under reduced pressure, and the resulting precipitate was collected by filtration. The solid was washed with diethyl ether and dried in vacuo to afford a yellow powder of complex **1**. Yield: 0.25 g (79%). ESI-MS: *m*/*z* 329.0 (calcd 329.1) [*M*/2 − 2NO$_3$ + OMe]$^+$. Anal. Calcd for C$_{28}$H$_{32}$Fe$_2$N$_{10}$O$_{14}$ (found): C, 39.83 (40.03); H, 3.82 (3.91); N, 16.59 (16.36). Single crystals of **1** suitable for X-ray diffraction were obtained by evaporation of the saturated methanol solution of **1**.

[Fe(L)(CAT)]$_2$ (2). A mixture of complex **1** (0.84 g, 1 mmol), catechol (0.22 g, 2 mmol), and triethylamine (0.50 g, 5 mmol) was stirred in methanol (15 mL) for 10 min. Upon vapor diffusion of diethyl ether to the resulting solution, dark-green crystals of **2**·2CH$_3$OH were obtained. ESI-MS: *m*/*z* 735.2 (calcd 735.2) [*M* − CAT + OMe]$^+$. Anal. Calcd for C$_{40}$H$_{40}$Fe$_2$N$_6$O$_6$ (found): C, 59.13 (58.98); H, 4.96 (4.89); N, 10.34 (10.29).

X-ray Crystallography. Crystallographic data were measured on a Siemens *SMART* System CCD diffractometer using graphite-monochromated Mo Kα radiation with a wavelength (λ) of 0.710 73 Å at a temperature of 293 ± 2 K. Data processing was accomplished with the *SAINT* processing program.[42] Intensity data were corrected for absorption by the *SADABS* program.[43] The structures were solved by direct methods and refined on F^2 against full-matrix least-squares methods using the *SHELXTL 97* program.[44] All non-hydrogen atoms were refined anisotropically. The hydrogen atoms were placed geometrically and held in the riding mode. Crystallographic data and processing parameters for complexes **1** and **2**·2CH$_3$OH are listed in Table 1.

Table 1. Crystallographic Data for **1** and **2**·2CH$_3$OH

	1	**2**·2H$_3$OH
formula	C$_{28}$H$_{32}$Fe$_2$N$_{10}$O$_{14}$	C$_{42}$H$_{48}$Fe$_2$N$_6$O$_8$
M_w	844.34	876.56
cryst syst	orthorhombic	monoclinic
space group	*Pbca*	$P2_1/c$
a, Å	14.126(3)	12.420(2)
b, Å	15.603(3)	19.090(3)
c, Å	15.496(3)	18.067(3)
α, deg	90.00	90.00
β, deg	90.00	105.644(2)
γ, deg	90.00	90.00
V, Å^3	3415. 4(12)	4125.1(11)
Z	4	4
ρ_{calcd}, g cm^{-3}	1.642	1.411
R1 [$I > 2\sigma(I)$][a]	0.0397	0.0507
wR2 [$I > 2\sigma(I)$][b]	0.1069	0.1396

[a] $R1 = (\sum||F_o| - |F_c||)/(\sum|F_o|)$. [b] $wR2 = [\sum w(F_o^2 - F_c^2)^2/\sum w(F_o^2)^2]^{1/2}$.

Spectrophotometric Titration. The spectrophotometric titration was performed as the reported procedure.[31,40,45] A methanol solution (20 μL) of H$_2$DBC (2 × 10^{-2} M, 1 equiv) was added to a solution of **1** (10^{-4} M) in methanol (2 mL). The resulting solution was titrated in portions of 0.2 equiv of piperidine (4 μL, 2 × 10^{-2} M in methanol), and the UV−vis spectra were monitored. To avoid the degradation of the catecolate adduct, the titration was operated under a dinitrogen atmosphere and repeated three times.

Catechol-Cleaving Activity. The catechol-cleaving dioxygenase activity of the complexes was explored in the methanol solution of the iron complex as described for spectrophotometric titration, except that the air-saturated methanol was used. The catecholate adduct was generated in situ upon the addition of 0.8 equiv of piperidine to the methanol solution of **1**. The decomposition of complex-substrate adducts was monitored by detecting the decay of the DBC^{2-}-to-iron(III) ligand-to-metal charge-transfer (LMCT) bands at 25 °C.

Studies of Cleavage Products. The oxidation products were determined by the following procedure similar to the literature method.[31,40] To a solution of complex **1** (0.07 mmol, 1.4 × 10^{-3} M) in methanol (50 mL) were added H$_2$DBC (0.14 mmol, 2.8 × 10^{-3} M) and 0.8 equiv of piperidine (0.11 mmol, 1.96 × 10^{-3} M). The reaction was carried out under 1 atm of oxygen at ambient temperature (25 °C). After 20 h, the resulting solution was concentrated under reduced pressure and the iron complexes were removed by silica gel column chromatography with CH$_2$Cl$_2$/CHCl$_3$ (1:1, v/v) as the eluent. After removal of the solvent, the products were dried in vacuo and identified by GC−MS and ^{1}H NMR spectroscopy.

Results and Discussion

Preparation of the Ligand and Iron Complexes. Ligand H**L** is analogous to *N*,*N*-bis(2-benzimidazolylmethyl)-*N*-(2-hydroxyethyl)amine, which was used as a ligand for the preparation of the mononuclear and μ-alkoxo dinuclear iron(III) complexes.[30,46,47] The deprotonated form of H**L** may act as an intramolecular base to mimic the function of Tyr447 in 3,4-PCD. Treatment of H**L** with Fe(NO$_3$)$_3$·9H$_2$O in methanol gave iron complex **1** as a yellow powder. Although

(41) Botha, J. M.; Umakoshi, K.; Sasaki, Y.; Lamprecht, G. J. *Inorg. Chem.* **1998**, *37*, 1609.
(42) Software packages *SMART* and *SAINT*; Siemens Energy & Automation Inc.: Madison, WI, 1996.
(43) Sheldrick, G. M. *SADABS Absorption Correction Program*; University of Göttingen: Göttingen, Germany, 1996.
(44) Sheldrick, G. M. *SHELXTL97 Program for the Refinement of Crystal Structure*; University of Göttingen: Göttingen, Germany, 1997.
(45) Xu, J.-Y.; Astner, J.; Walter, O.; Heinemann, F. W.; Schindler, S.; Merkel, M.; Krebs, B. *Eur. J. Inorg. Chem.* **2006**, 1601−1610.
(46) Ménage, S.; Que, L., Jr. *Inorg. Chem.* **1990**, *29*, 4293.
(47) Gao, E.-Q.; Yin, L.-H.; Tang, J.-K.; Cheng, P.; Liao, D.-Z.; Jiang, Z.-H.; Yan, S.-P. *Polyhedron* **2001**, *20*, 669.

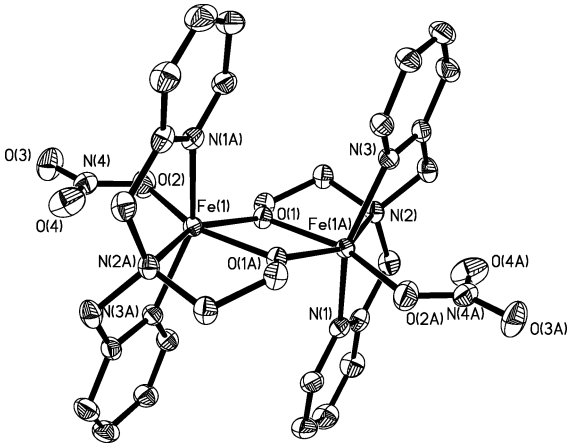

Figure 2. Molecular structure of the cation in **1** with thermal ellipsoids at 30% probability. All hydrogen atoms are omitted for clarity.

Table 2. Selected Bond Lengths (Å) and Angles (deg) for Complex **1**

Fe(1)−O(1)	1.958(2)	Fe(1)−N(1A)	2.084(2)
Fe(1)−O(1A)	2.013(2)	Fe(1)−N(2A)	2.223(2)
Fe(1)−O(2)	2.097(2)	Fe(1)−N(3A)	2.089(2)
O(1)−Fe(1)−O(1A)	72.23(8)	N(1A)−Fe(1)−O(2)	93.43(10)
O(1)−Fe(1)−N(1A)	106.21(8)	N(3A)−Fe(1)−O(2)	89.39(9)
O(1A)−Fe(1)−N(1A)	90.21(8)	O(1)−Fe(1)−N(2A)	150.60(8)
O(1)−Fe(1)−N(3A)	102.99(8)	O(1A)−Fe(1)−N(2A)	78.87(8)
O(1A)−Fe(1)−N(3A)	99.89(8)	N(1A)−Fe(1)−N(2A)	78.73(9)
N(1A)−Fe(1)−N(3A)	150.77(9)	N(3A)−Fe(1)−N(2A)	76.48(9)
O(1)−Fe(1)−O(2)	81.93(9)	O(2)−Fe(1)−N(2A)	127.21(9)
O(1A)−Fe(1)−O(2)	153.87(9)	Fe(1)−O(1)−Fe(1A)	107.77(8)

it is difficult to determine whether **1** is a mono- or binuclear complex based on the electrospray ionization MS (ESI-MS) and elemental analysis data, the single-crystal X-ray study reveals that **1** is a bis(μ-alkoxo)-bridged dinuclear iron(III) complex **1** in the solid state. The ESI-MS spectrum of the methanol solution of **1** does not show any peak for the binuclear complex, and only the peak derived from the mononuclear species $[Fe(\mathbf{L})(OMe)]^+$ can be found in the ESI-MS spectrum. This implies that the binuclear complex **1** is readily converted to a mononuclear species in a methanol solution. When complex **1** was reacted with catechol in the presence of excess triethylamine, a bis(μ-alkoxo)-bridged catecholate dinuclear complex **2** was obtained.

X-ray Crystal Structures of Complexes 1 and 2·2CH$_3$OH. The molecular structure of the dialkoxo-bridged binuclear complex **1** is shown in Figure 2. Selected bond lengths and angles are summarized in Table 2. Because of the centrosymmetry of the cation $[Fe(\mathbf{L})NO_3]_2^{2+}$, only half of the binuclear complex is found in an asymmetric unit. Each iron(III) center of **1** adopts a six-coordinate distorted octahedral configuration with an N_3O_3 donor set. The amine nitrogen and the bridged ethoxyl oxygen atoms lie in the plane of the Fe_2O_2 core. The pyridine nitrogen atoms occupy two axial positions in the octahedron. The oxygen atoms of the coordinate nitrate ions are trans to the ethoxyl bridges. The left coordination site is completed by the ethoxyl oxygen from the other **L** ligand. The Fe−N_{amine} bond length [2.223(2) Å] is considerably longer than the average length of the Fe−N_{py} bond [2.087(2) Å] as reported for the analogous diiron complexes containing the DBE ligand.[46] The uneven

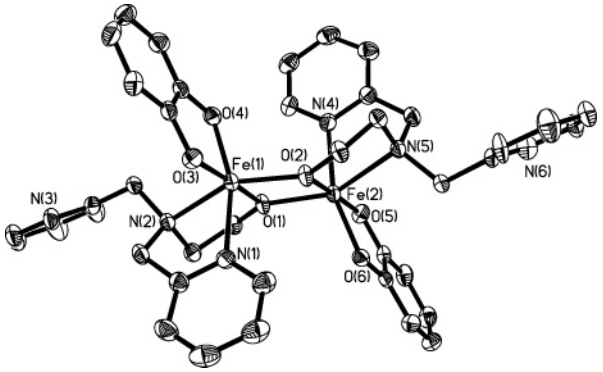

Figure 3. Molecular structure of **2** with thermal ellipsoids at 30% probability. All hydrogen atoms and solvent molecules (CH_3OH) in the lattice are omitted for clarity.

Table 3. Selected Bond Lengths (Å) and Angles (deg) for Complex **2**·2CH_3OH

Fe(1)−O(4)	1.939(2)	Fe(2)−O(5)	1.940(2)
Fe(1)−O(3)	1.964(2)	Fe(2)−O(6)	1.970(2)
Fe(1)−O(2)	1.975(2)	Fe(2)−O(1)	1.971(2)
Fe(1)−O(1)	2.017(2)	Fe(2)−O(2)	2.020(2)
Fe(1)−N(1)	2.189(3)	Fe(2)−N(4)	2.194(3)
Fe(1)−N(2)	2.268(3)	Fe(2)−N(5)	2.267(2)
O(4)−Fe(1)−O(3)	82.61(9)	O(5)−Fe(2)−O(6)	82.75(9)
O(4)−Fe(1)−O(2)	103.89(9)	O(5)−Fe(2)−O(1)	106.02(9)
O(3)−Fe(1)−O(2)	107.81(9)	O(6)−Fe(2)−O(1)	105.89(9)
O(4)−Fe(1)−O(1)	95.85(9)	O(5)−Fe(2)−O(2)	175.17(9)
O(3)−Fe(1)−O(1)	175.72(9)	O(6)−Fe(2)−O(2)	92.61(9)
O(2)−Fe(1)−O(1)	76.43(8)	O(1)−Fe(2)−O(2)	76.47(8)
O(4)−Fe(1)−N(1)	160.41(9)	O(5)−Fe(2)−N(4)	86.39(9)
O(3)−Fe(1)−N(1)	83.09(9)	O(6)−Fe(2)−N(4)	161.46(9)
O(2)−Fe(1)−N(1)	93.19(9)	O(1)−Fe(2)−N(4)	91.51(9)
O(1)−Fe(1)−N(1)	97.45(9)	O(2)−Fe(2)−N(4)	97.75(9)
O(4)−Fe(1)−N(2)	94.91(9)	O(5)−Fe(2)−N(5)	100.14(9)
O(3)−Fe(1)−N(2)	97.88(9)	O(6)−Fe(2)−N(5)	92.75(9)
O(2)−Fe(1)−N(2)	149.72(9)	O(1)−Fe(2)−N(5)	149.41(9)
O(1)−Fe(1)−N(2)	78.24(9)	O(2)−Fe(2)−N(5)	78.70(9)
N(1)−Fe(1)−N(2)	73.90(9)	N(4)−Fe(2)−N(5)	74.39(9)
Fe(1)−O(1)−Fe(2)	103.55(9)	Fe(1)−O(2)−Fe(2)	103.30(9)

distances of the Fe−O_{alkoxo} bonds [1.958(2) and 2.013(2) Å] are found in the asymmetric Fe_2O_2 core of **1** with Fe(1)−O(1)−Fe(1A) and O(1)−Fe(1)−O(1A) angles of 107.77(8) and 72.23(8)°, respectively. As expected, the large O(2)−Fe(1)−N(2A) angle [127.21(9)°] is observed, which allows a weak interaction between the other nitrate oxygen atom and the iron atom [Fe(1)−O(4) 2.622 Å] in addition to the Fe(1)−O(2) bond [2.097(2) Å]. The Fe(1)···Fe(1A) separation (3.208 Å) of **1** is close to those observed for $[Fe_2(DBE)_2(OBz)_2](ClO_4)_2$ [3.21(1) Å] and $[Fe_2(DBE)_2(N_3)_2](ClO_4)_2$ (3.196 Å).[46,47]

The unit cell of **2** consists of four complexes and eight methanol molecules. The molecular structure of **2** is shown in Figure 3, and the selected bond lengths and angles are given in Table 3. The structural feature of **2** resembles its parent complex **1**. Complex **2** possesses an asymmetric Fe_2O_2 core, in which two iron atoms are bridged by the ethoxyl oxygen atoms of the ligands. The distances of the Fe−O_{alkoxo} bonds are in the range of 1.971(2)−2.020(2) Å, and the Fe−O−Fe and O−Fe−O angles of the Fe_2O_2 core are 76.43(8), 76.47(8), 103.30(9), and 103.55(9)°. The hydrogen bond between the methanol molecule in the lattice and the O(3) atom leads to the subtle difference in coordination of the

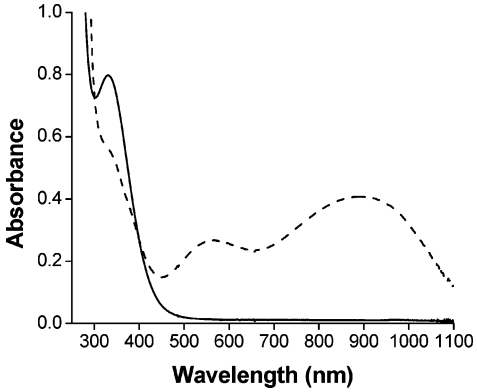

Figure 4. UV−vis spectra of **1** (—) and its catecholate adduct **1**-DBC (- - -) (2×10^{-4} M based on Fe^{3+}) in methanol.

two catecholate dianions and consequently results in the asymmetric structure of complex **2**. A similar structure was also found in the binuclear complex [{Fe(APEA)(tcc)}$_2$(μ-O)] [tcc = tetrachlorocatechol; APEA = *N*-acetyl-*N*,*N*′-bis-(2-pyridylmethyl)ethylenediamine] containing two catecholate dianions,[45] in which two iron atoms are linked by a μ-oxo bridge. Each iron atom of **2** is in a six-coordinate pseudooctahedral environment with an N_2O_4 donor set, constituted by an ethoxyl oxygen, a pyridine nitrogen, and an amino nitrogen from one of the **L** ligands and two phenolate oxygen atoms of catechol as well as an ethoxyl oxygen from the other **L** ligand. One of the pyridyl arms of the ligand **L** is left uncoordinated. The dihedral angles between the pendent pyridine ring and the catecholate plane in each iron flank are 83.5 and 83.9°. The Fe(1)−Fe(2) distance of 3.133 Å corresponds to the value found in the analogous dialkoxo-diiron complexes.[48] The average Fe−N_{py} bond length (2.192 Å) is shorter than the Fe−N_{amine} bond (2.268 Å). The cis angles around each iron center are in the range of 73.90-(9)−107.81(9)°, greatly deviating from 90° for a standard octahedral coordination geometry. The large cis angles between the catecholate oxygen and the bridged ethoxyl oxygen [O(4)−Fe(1)−O(2), O(3)−Fe(1)−O(2), O(5)−Fe-(2)−O(1), and O(6)−Fe(2)−O(1), 103.89(9)−107.81(9)°] are observed in complex **2**.

Electronic Spectra. The UV−vis spectra of complex **1** and its DBC^{2-} adduct (Figure 4) were measured in methanol. Complex **1** shows an intense LMCT transition band at 330 nm ($\epsilon = 3990\ M^{-1}\ cm^{-1}$), probably arising from the charge transfer of the methoxyl or ethoxyl oxygen to the iron(III) center.[49−52] Under this condition, the ESI-MS spectrum of **1** shows the peak at *m*/*z* 329.0 (100%), corresponding to the mononuclear species [Fe(**L**)(OMe)]$^+$ (calcd 329.1). This suggests that diiron complex **1** exists as a mononuclear species in a methanol solution and the ethoxyl arm cannot be protonated by methanol.

Formation of the mononuclear complex-substrate adduct is essential for the catechol intradiol cleavage.[1,2] The catecholate adduct of complex **1**, formed by the reaction of the complex and H_2DBC in methanol in the presence of 0.8 equiv of piperidine, was detected in situ by UV−vis spectroscopy (Figure 4). Two new visible bands with maximum absorption at 560 ($\epsilon = 1330\ M^{-1}\ cm^{-1}$) and 910 nm ($\epsilon = 2030\ M^{-1}\ cm^{-1}$), were observed for the catecholate adduct of complex **1**, which are attributed to DBC^{2-}-to-iron(III) LMCT transitions involving two different catecholate ligand orbitals.[26,27,33,34,37,38] As reported in many cases, the energy of the LMCT transitions strongly depends on the nature of the ligands, and it reflects the Lewis acidity of the iron center in the complex.[24] The **1**-DBC adduct shows LMCT bands at 560 and 910 nm, implying a relatively strong acidity of the iron center. It is reported that the in situ generated DBC^{2-} adduct [Fe(APEA)(DBC)]$^+$ exhibited two intense catecholate-to-iron(III) LMCT bands at 580 and 920 nm,[45] which are very close to the bands observed for **1**-DBC, suggesting a similar coordination sphere involved in the two complexes. On the basis of these arguments, we propose that the **L** ligand in the **1**-DBC adduct adopts an all-π-coordinate mode. Repeated attempts to isolate the intermediate **1**-DBC for structure determination were not successful, but the ESI-Q-TOF spectrum of **1**-DBC in methanol shows a peak at *m*/*z* 519.1553 for [Fe(H**L**)(DBC)]$^+$ species (100%, calcd 519.2184), giving further evidence for the formation of the catecholate adduct with the ethoxyl arm protonated by catechol.

Furthermore, studies on the oxidation reaction of **1**-DBC and dioxygen in methanol (vide infra) display no extradiol cleavage products formed, indicating that there is no vacant coordination site available for binding dioxygen on the iron center.[53−56] According to the above analysis, the possible structure of [Fe(H**L**)(DBC)]$^+$ is described as **B** in Scheme 1, in which H**L** servers as the tetradentate ligand with an ethanol arm coordinating to the iron center.

The important issue here is that the UV−vis and MS spectra of **1**-DBC indicate that the ethoxyl moieties of complex **1** are capable of accepting the protons from catechol. In this viewpoint, in addition to the previously reported exogenous ligand acac[33] and the bromopyridyl moiety of ligand BrTPA,[40] the ethoxyl moiety of the tripodal N_3O ligand is another type of functional model for Tyr447 in 3,4-PCD in the first step of the catechol intradiol cleavage cycle.

Spectrophotometric Titration. To attain the high concentration of the mononuclear iron(III) catecholate adduct and the high catechol cleavage activity, the optimal condition for complex **1** was determined by spectrophotometric titration. The titration spectrum (Figure 5) was obtained by the

(48) Kurtz, D. M., Jr. *Chem. Rev.* **1990**, *90*, 585.
(49) Jonas, R. T.; Stack, T. D. P. *J. Am. Chem. Soc.* **1987**, *119*, 8566.
(50) Roelfes, G.; Lubben, M.; Chen, K.; Ho, R. Y. N.; Meetsma, A.; Genseberger, S.; Hermant, R. M.; Hage, R.; Mandal, S. K.; Young, V. G., Jr.; Zang, Y.; Kooijman, H.; Spek, A. L.; Que, L., Jr.; Feringa, B. L. *Inorg. Chem.* **1999**, *38*, 1929.
(51) Duelund, L.; Hazell, R.; McKenzie, C. J.; Nielsen, L. P.; Toftlund, H. *J. Chem. Soc., Dalton Trans.* **2001**, 152.
(52) Taktak, S.; Kryatov, S. V.; Rybak-Akimova, E. V. *Inorg. Chem.* **2004**, *43*, 7196.
(53) Jo, D.-H.; Chiou, Y.-M.; Que, L., Jr. *Inorg. Chem.* **2001**, *40*, 3181.
(54) Jo, D.-H.; Que, L., Jr. *Angew. Chem., Int. Ed.* **2000**, *39*, 4284.
(55) Lin, G.; Reid, G.; Bugg, T. D. H. *J. Am. Chem. Soc.* **2001**, *123*, 5030.
(56) Mayilmurugan, R.; Suresh, E.; Palaniandavar, M. *Inorg. Chem.* **2007**, *46*, 6038.

Scheme 1. Proposed Pathway for the Formation of Catecholate Adduct $[Fe(H\mathbf{L})(DBC)]^+$

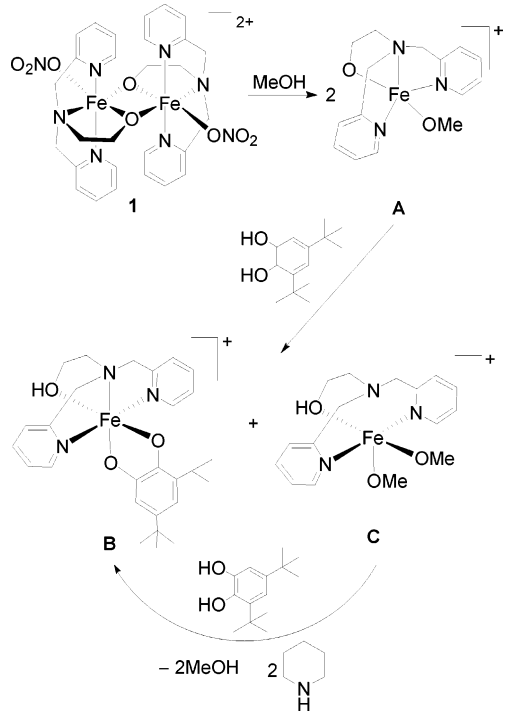

addition of piperidine in portions to the methanol solution of 0.5 equiv of **1** and 1 equiv of H_2DBC. The intense absorption band at 375 nm in the absence of a base is tentatively attributed to the LMCT band for $[Fe(H\mathbf{L})(OMe)_2]^+$ (species **C**, Scheme 1), and the bands at 560 and 910 nm are assigned to the LMCT bands of the catecholate adduct $[Fe(H\mathbf{L})(DBC)]^+$ (species **B**).

The ESI-Q-TOF spectrum of the above solution shows two peaks at *m*/*z* 361.0281 and 519.1553 (Figure S1 in the Supporting Information). In terms of the ready split of the μ-oxo bridge of the diiron complex in a polar solvent, we assume that the peak at *m*/*z* 361.0281 corresponds to $[Fe(H\mathbf{L})(OMe)_2]^+$ species (calcd 361.1089), which is derived from the reaction of the μ-oxo-bridged diiron complex $[\{Fe(H\mathbf{L})(NO_3)\}_2(\mu\text{-}O)]^{2+}$ and methanol. The peak at *m*/*z* 519.1553 is assigned to the mononuclear species $[Fe(H\mathbf{L})(DBC)]^+$ (calcd 519.2184). Based on these results, it can be deduced that the ethoxyl moiety of ligand **L** in both species is protonated.

Upon successive addition of piperidine, the band at 375 nm gradually disappeared and the intensities of the bands at 560 and 910 nm dramatically increased. The maximum intensity was attained by the addition of 0.8 equiv of piperidine, indicating the highest concentration of the mononuclear adduct.

Further addition of piperidine resulted in two new absorption bands at 450 (shoulder) and 700 nm, accompanied by the disappearance of the LMCT bands of the mononuclear catecholate adduct. After 1.8 equiv of base was added, the bands at 450 and 700 nm reached their highest intensities and did not change with further addition of the base. In light of the structure of complex **2**, which was obtained under the same conditions except that the substrate H_2DBC was

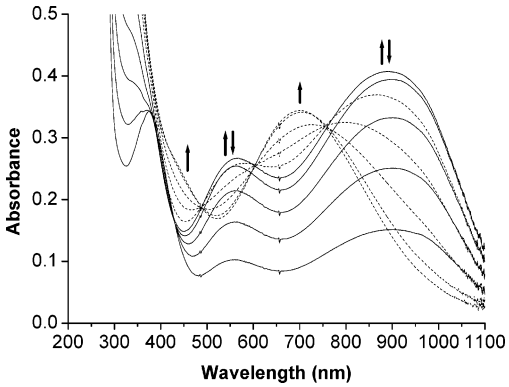

Figure 5. Spectrophotometric titration of the methanol solution of **1** (0.5 equiv) and H_2DBC (1 equiv) with different amounts of piperidine: 0−0.8 equiv (—); 1.0−1.8 equiv (···).

replaced by catechol, it could be deduced that the two new bands at 450 and 700 nm belong to the μ-oxo-bridged diiron complex $[Fe(\mathbf{L})(DBC)]_2$, which are assigned to DBC^{2-}-to-iron(III) LMCT transitions from different catecholato orbitals. The iron complex similar to **2** was also observed in the iron(III)/APEA system.[45] Furthermore, we found that the binuclear catecholate adduct **2** did not show catechol cleavage activity.

According to the results of spectrophotometric titration, the following conversion process is suggested (Scheme 1). Upon the addition of H_2DBC to the solution of complex **1**, concerted reactions of proton transfer and ligand exchange occur. The ethoxyl group is quickly protonated by H_2DBC because of the strong binding ability of the catecholate dianion, and the catecholate dianion is coordinated to the iron(III) center to generate the active mononuclear adduct. With the addition of base, the acidity of the solution is adjusted, resulting in fast deprotonation of H_2DBC and in complete conversion of other intermediates (**A** and **C**) to the mononuclear catecholate adduct **B**. Further addition of piperidine leads to deprotonation of the ethanol moiety in the mononuclear adduct to generate an inert μ-alkoxo-bridged diiron complex with a structure similar to that of **2**.

The results of spectrophotometric titration and MS corroborate a spontaneous proton transfer from substrate to ligand. A quite small amount of external base (0.8 equiv based on Fe^{3+}) is required for complex **1** to attain the highest concentration of the active adduct. It is noteworthy that the base demanded for the optimal condition in the present system is lower than the required amount reported for other iron(III) systems (1.3−2.5 equiv),[31,40,45,57] indicating that the ethoxyl moiety of **L** can be used as an effective functional model of Tyr447 in 3,4-PCD. Although the titration spectrum of complex **1** is similar to that of the iron(III)/APEA system, the in situ generated iron species bearing the ligand APEA with a carboxamide arm is incapable of accepting the protons from the catechol substrate.[45] Consequently, the amount of base demanded for the iron(III)/APEA system to attain the highest concentration of the mononuclear catecholate adduct is 0.9 equiv more than that needed by the system of complex

(57) Merkel, M.; Pascaly, M.; Krebs, B.; Astner, J.; Foxon, S. P.; Schindler, S. *Inorg. Chem.* **2005**, *44*, 7582.

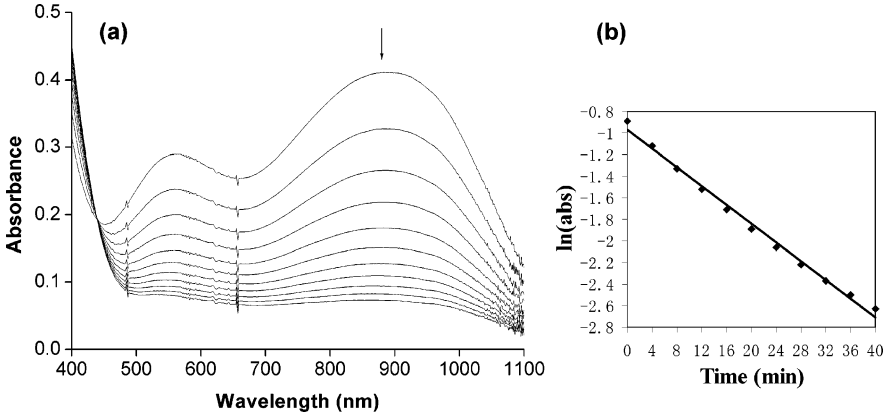

Figure 6. (a) Reaction progress of $[Fe(HL)(DBC)]^+$ (2×10^{-4} M) with dioxygen in an air-saturated methanol solution at 25 °C (interval: 4 min). (b) Plot of ln(abs) vs time based on absorption changes at 910 nm.

Scheme 2. Oxidation Products of H_2DBC

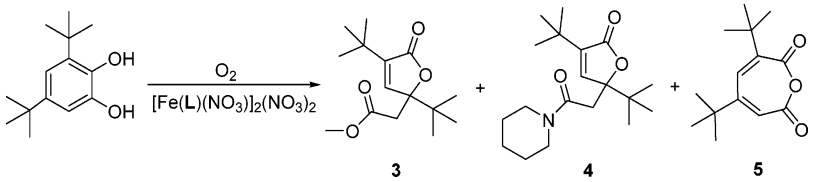

1. It means that the ethoxyl moiety of ligand **L** can act as 0.9 equiv of the external base, which is close to the theoretical amount of 1.0 equiv base. A very interesting system was reported recently by Funabiki et al. for the μ-oxo binuclear complex $[Mn(TPA)(\mu\text{-}O)]_2^{2+}$, which was capable of quantitatively accepting the protons of H_2DBC to form $[Mn(TPA)(DBC)]^+$ and H_2O in methanol without the addition of an external base.[58] This result gives further evidence that aerobic oxidation of catechols promoted by transition-metal complexes bearing the internal-base ligand can be carried out by the addition of a relatively small amount of base or even without an external base. In comparison to Funabiki's Mn/TPA system, the present Fe**L** system has the following differences: (1) The bridging oxygen in complex $[Mn(TPA)(\mu\text{-}O)]_2^{2+}$ is an exogenous ligand, while the ethoxyl arm in complex **1** is one part of the primary ligand, which is used to functionally mimic not only the Tyr447 unit but also the other structural character of 3,4-PCD. (2) The complex $[Mn(TPA)(\mu\text{-}O)]_2^{2+}$ promotes the oxidation of H_2DBC, acting as a catechol oxidase model to exclusively give quinone products. In contrast, the complex $[Fe(\mathbf{L})(NO_3)]_2^{2+}$ promotes the intradiol cleavage oxidation of H_2DBC, performing as a catechol dioxygenase model.

Intradiol Cleavage Activity. The catechol dioxygenase activity of complex **1** was investigated by monitoring the decay of the low-energy LMCT bands of the in situ generated DBC^{2-} adducts in an air-saturated methanol solution at ambient temperature. The activity of complex **1** was first explored by the UV−vis spectral change with the addition of 0.8 equiv of piperidine to the mixture of 0.5 equiv of the iron complex and 1 equiv of H_2DBC to obtain the highest reactivity (Figure 6a). The plot (Figure 6b) of ln(abs) vs time indicates that the reaction of $[Fe(HL)(DBC)]^+$ with dioxygen under these conditions is pseudo-first-order. The value of k_{obs} is deduced from the slope of the linear graph as 8.06×10^{-4} s^{-1}, and the reaction rate constant k is 0.38 M^{-1} s^{-1} in terms of $[O_2] = 2.12 \times 10^{-3}$ M in air-saturated methanol at 25 °C ($k = k_{obs}/[O_2]$).[31] The reaction rate of $[Fe(HL)(DBC)]^+$ with dioxygen is much faster than those reported for the iron(III) system of the ligand APEA with a weak coordinate acetyl moiety in the ligand ($k = 0.05$ M^{-1} s^{-1})[45] and $[Fe(DBE)(DBC)]^{2+}$ containing the similar ligand with an ethanol moiety ($k = 0.046$ M^{-1} s^{-1}).[30] The reaction rate of $[Fe(HL)(DBC)]^+$ is comparable to those for the complexes $[Fe(TPEA)(DBC)]^+$ [$k = 0.28$ M^{-1} s^{-1}; TPEA = *N*-methyl-*N*,*N*′,*N*′-tris(2-pyridylmethyl)ethylenediamine][59] and $[Fe(DDP)(DBC)]^+$ [$k = 0.38$ M^{-1} s^{-1}; DDP = *N*,*N*′-dimethyl-2,11-diaza[3.3](2,6)pyridinophane][60] containing N_4 coordinate ligands, and it is lower than those observed for the iron(III)/BrTPA system ($k = 1.3$ M^{-1} s^{-1})[40] and $[Fe(TPA)(DBC)]^+$ ($k = 10$ M^{-1} s^{-1}).[19,57] An attractive characteristic of the present system is its low demand of base for attaining high reactivity of the catecholate adduct. To confirm the results of spectrophotometric titration, the reaction rates were also measured under different amounts of piperidine, and it is found that the maximum reaction rate was obtained by the addition of 0.8 equiv of base.

Determination of the Oxidation Products. The oxidation products of $[Fe(HL)(DBC)]^+$ in the stoichiometric reaction were identified by GC−MS, and the yields of the products were determined by ^1H NMR spectra with integration of the signals of the aromatic ring in the range of δ 6−7 (Figure S2 in the Supporting Information). After the reaction ran for 20 h, the major products were determined as intradiol cleavage products in 83.9% yield (Scheme 2), composed of

(58) Hitomi, Y.; Ando, A.; Matsui, H.; Ito, T.; Tanaka, T.; Ogo, S.; Funabiki, T. *Inorg. Chem.* **2005**, *44*, 3473.

(59) Mialane, P.; Tchertanov, L.; Banse, F.; Sainton, J.; Girerd, J.-J. *Inorg. Chem.* **2000**, *39*, 2440.

(60) Koch, W. O.; Krüger, H.-J. *Angew. Chem., Int. Ed. Engl.* **1995**, *34*, 2671.

52.6% of (2,4-di-*tert*-butyl-5-oxo-2,5-dihydrofuran-2-yl)-acetic acid methyl ester (**3**) and 31.3% of 3,5-di-*tert*-butyl-5-(2-oxo-2-piperidinylethyl)-5*H*-furanone (**4**). Although the *cis*,*cis*-muconic anhydride, which was observed in many cases of intradiol cleavage oxidation,[19,30,33,37,40,61] was not detected after a long reaction time, it was observed by GC analysis when the reaction time was shortened. It is reasonable to postulate that the furanone products are derived by the nucleophilic attack of methanol and piperidine to the intermediate anhydride and by the sequential cyclization.[25] The autoxidation product of 3,5-di-*tert*-butyl-1,2-benzoquinone (**5**) was also detected as a minor product (16.1%).

Conclusions

The bis(μ-alkoxo)-bridged dinuclear iron(III) complex **1** of the tripodal N_3O ligand and its catechol adduct **2** were prepared and structurally characterized. Complex **1** displays catechol intradiol-cleaving dioxygenase activity. The UV−vis and MS spectra show that the ethoxyl moieties of diiron complex **1** can act as an internal base to accept protons from the catechol substrate, forming an active mononuclear iron(III) species $[Fe(H\mathbf{L})(DBC)]^+$. Therefore, a relatively small amount of external base (0.8 equiv based on Fe^{3+}) is needed to attain the highest dioxygenase activity. The reaction rate of $[Fe(H\mathbf{L})(DBC)]^+$ with dioxygen in an air-saturated methanol solution at 25 °C is 0.38 M^{-1} s^{-1}. The ethoxyl moiety of the tripodal N_3O ligand (**L**) is an effective functional model for Tyr447 in 3,4-PCD.

Acknowledgment. We are grateful to the Chinese National Natural Science Foundation (Grants 20471013 and 20633020), the Swedish Energy Agency, the Swedish Research Council, and the K&A Wallenberg Foundation for financial support of this work.

Supporting Information Available: Crystallographic information files (CIF) for complexes **1** and **2**·2CH_3OH, the ESI-Q-TOF mass spectrum resulting from the addition of H_2DBC into the methanol solution of complex **1**, and the ^1H NMR spectrum of the product mixture from the catalytic reaction. This material is available free of charge via the Internet at http://pubs.acs.org.

IC700664U

(61) Panja, A.; Goswami, S.; Shaikh, N.; Roy, P.; Manassero, M.; Butcher, R. J.; Banerjee, P. *Polyhedron* **2005**, *24*, 2921.